

Structural Basis for Pterin Antagonism in Nitric-oxide Synthase

DEVELOPMENT OF NOVEL 4-OXO-PTERIDINE ANTAGONISTS OF (6R)-5,6,7,8-TETRAHYDROBIOPTERIN*

Received for publication, December 20, 2000, and in revised form, October 1, 2001
Published, JBC Papers in Press, October 5, 2001, DOI 10.1074/jbc.M011469200

Peter Kotsonis‡, Lothar G. Fröhlich, C. S. Raman§, Huiying Li¶, Michael Berg||, Rainer Gerwig||, Viola Groehn||, Yonghan Kang||, Najim Al-Masoudi||, Shahriyar Taghavi-Moghadam||, Detlev Mohr||, Ursula Münch||, Joachim Schnabel||, Pavel Martásek**, Bettie S. S. Masters**, Hartmut Strobel‡‡, Thomas Poulos¶, Hans Matter‡‡, Wolfgang Pfeleiderer||, and Harald H. H. W. Schmidt§§

From the Department of Pharmacology and Toxicology, Julius-Maximilians University, Versbacher Straße 9, Würzburg 97078, Germany, the §Structural Biology Center MSB 6.128, Department of Biochemistry and Molecular Biology, University of Texas Medical School, Houston, Texas 77030, the ¶Department of Molecular Biology and Biochemistry, Program in Macromolecular Structure, University of California, Irvine, California 92697, the ||Faculty of Chemistry, University of Konstanz, Konstanz 78434, Germany, the **Department of Biochemistry, University of Texas Health Science Center, San Antonio, Texas 78229, and ‡‡Aventis Pharma, Research Chemistry Frankfurt, Building G838, Frankfurt 65926, Germany

Pathological nitric oxide (NO) generation in sepsis, inflammation, and stroke may be therapeutically controlled by inhibiting NO synthases (NOS). Here we targeted the (6R)-5,6,7,8-tetrahydro-L-biopterin (H₄Bip)-binding site of NOS, which, upon cofactor binding, maximally increases enzyme activity and NO production from substrate L-arginine. The first generation of H₄Bip-based NOS inhibitors employed a 4-amino pharmacophore of H₄Bip analogous to antifolates such as methotrexate. We developed a novel series of 4-oxo-pteridine derivatives that were screened for inhibition against neuronal NOS (NOS-I) and a structure-activity relationship was determined. To understand the structural basis for pterin antagonism, selected derivatives were docked into the NOS pterin binding cavity. Using a reduced 4-oxo-pteridine scaffold, derivatives with certain modifications such as electron-rich aromatic phenyl or benzoyl groups at the 5- and 6-positions, were discovered to markedly inhibit NOS-I, possibly due to hydrophobic and electrostatic interactions with Phe⁴⁶² and Ser¹⁰⁴, respectively, within the pterin binding pocket. One of the most effective 4-oxo compounds and, for comparisons an active 4-amino derivative, were then co-crystallized with the endothelial NOS (NOS-III) oxygenase domain and this structure solved to confirm the hypothetical binding modes. Collectively, these findings suggest (i) that, unlike the antifolate principle, the 4-amino substituent is not essential for developing pterin-based NOS inhibitors and (ii), provide a steric and electrostatic basis for their rational design.

Inhibitors of nitric-oxide synthase (NOS¹; EC 1.14.13.39) have been developed as therapeutic agents to modulate pathologically high nitric oxide (NO) synthesis (1, 2). The family of NOS catalyzes the oxidation of substrate L-arginine to L-citrulline and NO (3–5), or a related molecule (6–8), in an NADPH and O₂-dependent manner (9). Enzyme activity depends on multiple cofactors including FAD, FMN, (6R)-5,6,7,8-tetrahydro-L-biopterin (H₄Bip), and iron protoporphyrin IX (heme), which are localized within each by-domain monomer consisting of an N-terminal oxygenase and a C-terminal reductase domain connected by a calmodulin (CaM) recognition sequence (10–14). Importantly, only homodimeric NOS is able to metabolize L-arginine and a single intersubunit ZnS₄ cluster appears to be important for stabilizing the dimer and H₄Bip-binding site (10, 15, 16). To date, three distinct isoforms of NOS (9, 10) have been identified: these include NOS-I (nNOS or neuronal) and NOS-III (eNOS or endothelial), which are constitutively expressed and Ca²⁺-dependent. The former is localized in neurons, skeletal muscle, epithelial cells and modulates neurotransmission, gastrointestinal motility, and penile erection (9, 17, 18), while NOS-III is found in vascular endothelial cells (19) and regulates blood pressure homeostasis (20, 21). The so-called “inducible” NOS-II isoform (or iNOS) is expressed in a number of tissues in response to endotoxin/cytokines and plays a role in the immune response (2, 22); its activity does not depend on physiological changes in free intracellular Ca²⁺. Finally, for two of the isoforms, NOS-II and III, structural information is available from x-ray crystallography studies using recombinantly expressed NOS oxygenase domain which show highly conserved cofactor and substrate binding modes (15, 16, 23).

Overproduction of NO by NOS-I and II has been implicated in various pathological conditions including sepsis, inflammation, stroke, and neurodegenerative diseases (2, 9). To date, a wide variety of NOS inhibitors have been developed as therapeutic candidates and used in both animal models and, to a lesser extent, in humans (1, 2). Prototypical compounds were mainly analogs of the substrate L-arginine (24–26) such as N^ω-methyl-L-arginine, which in clinical trials reversed the hy-

* This work was supported in part by the Bundesministerium für Bildung, Wissenschaft, Forschung und Technologie (BMBF), and Aventis Pharma AG (Germany). The costs of publication of this article were defrayed in part by the payment of page charges. This article must therefore be hereby marked “advertisement” in accordance with 18 U.S.C. Section 1734 solely to indicate this fact.

The atomic coordinates and structure factors (code 1DMJ) have been deposited in the Protein Data Bank, Research Collaboratory for Structural Bioinformatics, Rutgers University, New Brunswick, NJ (<http://www.rcsb.org/>).

‡ Recipient of a C. J. Martin fellowship (Australian NH MRC) and was supported by vasopharm BIOTECH GmbH (Germany). To whom correspondence should be addressed: Novartis Institute for Medical Sciences, 5 Gower Place, London WC1E 6BS, UK. Tel.: 44-20-7387-4445; Fax: 44-20-7387-4116; E-mail: peter.kotsonis@pharma.novartis.com.

§§ Present address: Justus-Liebig-University, Rudolf-Buchheim Institute for Pharmacology, Frankfurter Straße 107, 35392 Giessen, Germany. E-mail: Harald.Schmidt@pharma.med.uni-giessen.de.

¹ The abbreviations used are: NOS, nitric-oxide synthase enzyme family (EC 1.14.13.39); H₄Bip, (6R)-5,6,7,8-tetrahydro-L-biopterin; IC₅₀, value, concentration of inhibitor required for half-maximal inhibition; NO, nitric oxide (synonym nitrogen monoxide); SCR, structurally conserved region; Chapso, 3-[(3-cholamidopropyl)-dimethylammonio]-2-hydroxy-1-propanesulfonate.

potension due to sepsis but did not increase survival (1, 2). However, substrate-based inhibitors, which may also interfere with other L-arginine-dependent biological pathway(s), have failed to succeed in clinical development (1, 2). Interestingly, although the NOS co-product L-citrulline does not regulate NOS activity (8), analogs of L-citrulline such as L-thiocitrulline have been reported to be potent NOS inhibitors although only developed pre-clinically (1, 27–29).

Other binding sites of NOS have been pharmacologically targeted including the flavin cofactor sites (FMN and FAD) within the reductase domain (1, 30–32, 72). Potent and irreversible inhibitors such as diphenyleneiodonium (IC_{50} of 50–150 nM) interfere with flavin function (1). However, given the ubiquitous distribution of NADPH-dependent flavoproteins within the body, the use of diphenyleneiodonium may be of limited value. NOS catalysis can be inhibited within the oxygenase domain by compounds binding to the heme prosthetic group such as indazoles and imidazoles (33, 34). However, the specificity of various indazoles and imidazoles for the heme-binding site is questionable.

A more promising target within NOS is the H_4 Bip-binding site, which, upon cofactor binding markedly increases NOS activity or stability and, consequently NO synthesis (35–39). This site differs structurally compared with other pterin-dependent enzymes such as the aromatic amino acid hydroxylases (35–40). We recently described prototypical pterin-based inhibitors that were optimized for NOS-I inhibition and did not interfere with phenylalanine hydroxylase (38, 40). Interestingly, a 4-amino analog of H_4 Bip was also reported to be a potent inhibitor of H_4 Bip function in NOS (38, 41) and various substituted derivatives demonstrated similar efficacy (42). This suggested a close similarity between anti-pterin inhibitors of NOS and antifolate inhibitors of dihydrofolate reductase since both chemical scaffolds appeared to require a 4-amino functionality to inhibit their target enzyme. However, due to structural similarities with tetrahydrofolic acid, 4-amino H_4 Bip additionally inhibits dihydropteridine and folate reductases (40) and, therefore, other 4-amino analogs may also lack selectivity for NOS.

Herein we synthesized and refined a novel series of pterin-based NOS inhibitors based on an intact 4-oxo-pteridine nucleus analogous to the naturally occurring H_4 Bip. By systematically varying the substitution patterns in the 2-, 4-, 5-, 6-, and 7-positions of the 4-oxo-pteridine nucleus, these compounds were discovered to be effective NOS inhibitors and we here describe their structure-activity relationship. Importantly, docking studies with the most effective inhibitors led to a better understanding of the molecular considerations underlying NOS inhibition and was supported by co-crystallization within the largely conserved NOS-III oxygenase domain. These findings indicate that, unlike the antifolates, the 4-amino moiety is not a structural prerequisite for NOS inhibition thus allowing for the design of inhibitors with greater NOS selectivity. Collectively, this information provides a molecular basis for the rational design and optimization of novel, pteridine-based NOS inhibitors.

EXPERIMENTAL PROCEDURES

Materials—L-[2,3,4,5- 3 H]Arginine hydrochloride (2.85 TBq mmol $^{-1}$) was purchased from Amersham Pharmacia Biochem (Braunschweig, Germany); NADPH from AppliChem (Darmstadt, Germany); reduced glutathione (GSH) from Roche Molecular Biochemicals (Mannheim, Germany); (6R)-5,6,7,8-tetrahydro-L-biopterin (H_4 Bip) from Dr. Schircks Laboratories (Jona, Switzerland); FAD, FMN, L-arginine hydrochloride, and phosphodiesterase 3',5'-cyclic nucleotide activator (calmodulin, CaM) from Sigma (Deisenhofen, Germany). All 4-oxo-pteridine derivatives were synthesized in the Faculty of Chemistry, University of Konstanz (Germany) and purified by either re-crystallization or by chro-

matographic means (at >98% purity as determined by TLC and NMR spectra) and, characterized by 1 H NMR, UV/vis, and elemental analysis. All tetrahydropteridine derivatives in Table I were synthesized by catalytic reduction and isolated as either pure (2–8), or as racemic (1, 11–18) and diastereoisomeric mixtures (9, 10). Detailed synthetic procedures will be published elsewhere except for derivatives 19 (see Refs. 43 and 44) and 1, 14–17, 20, and 21 (see Ref. 45). All other chemicals, reagents, and solvents were of the highest purity available and either from Merck AG (Darmstadt, Germany) or Sigma (Deisenhofen, Germany). Water was deionized to 18 M Ω (Milli-Q; Millipore, Eschborn, Germany). Unless otherwise indicated, all chemicals were dissolved in Argon de-oxygenated water.

Enzyme Activity—Native NOS-I was isolated from porcine brain cerebellum by previously described methods (38, 42, 46). The yield of this purification method (42) was 0.5 mg of enzyme from 1.0 kg of tissue with greater than 90% purity (from densitometric scanning of Coomassie-stained SDS-polyacrylamide electrophoresis gels) and a specific activity of up to 670 nmol of L-citrulline mg $^{-1}$ min $^{-1}$. Native NOS-I is known to co-purify with substoichiometric amounts of bound H_4 Bip and basal enzyme activity (residual activity in the absence of exogenously added H_4 Bip) was 10–40% of V_{max} (total activity in the presence of excess, exogenously added H_4 Bip). Basal NOS-I activity is considered to be independent of bound pterin following purification (38, 42). Catalytic activity of NOS-I was determined from the Ca $^{2+}$ /calmodulin-dependent conversion of L-[3 H]arginine to L-[3 H]citrulline (11, 46) during a standard incubation of 15 min (at 37 °C) with the following assay mixture (volume of 100 μ l, pH 7.2); NOS-I (0.4 μ g), 50 nM CaM, 1 mM CaCl $_2$, 5 μ M FAD, 10 μ M FMN, 250 μ M Chapso, 50 mM triethanolamine, 1 mM NADPH, 7 mM GSH, 50 μ M total L-arginine of L-[2,3,4,5- 3 H]arginine and 2 μ M H_4 Bip. The reaction was stopped by adding ice-cold acetate buffer (pH 5.5). The L-[3 H]citrulline formed was separated by cation exchange chromatography and the amount of radioactivity determined by liquid scintillation counting.

To identify active compounds,² we initially examined the effects of the derivatives on H_4 Bip-stimulated NOS-I activity at a single concentration of 100 μ M. Those derivatives identified as being active (>50% inhibition of H_4 Bip-stimulated NOS activity) were re-screened over a full concentration range (0–1000 μ M) to determine accurate log(concentration)-response relationships and establish potency (IC_{50}). The corresponding IC_{50} values were determined by nonlinear regression analysis using either Biosoft UltraFit software (Cambridge, United Kingdom) or GraphPad Prism software (San Diego, CA). Individual curves from each triplicate were fitted by nonlinear regression analysis to sigmoidal concentration-response curves of variable slope (that is, the Hill slope was not fixed equal to 1). The corresponding IC_{50} value from each curve was then calculated by the software and is represented as means.

Computational Procedures—All modeling work was done using the program package SYBYL (47) on Silicon Graphics workstations. All energy calculations of protein-ligand complexes were based on the TRI-POS 6.0 force field (48) using Gasteiger-Marsili charges (49). Initial conformations of ligands and complexes were minimized using quasi-Newton-Raphson (BFGS) or conjugate gradient algorithms for 5000 steps. For docking of candidate molecules, the public x-ray structures of endothelial and inducible NOS isoforms were used (15, 50). For the

² The screening methodology and data analysis used here were similar to our previous work (38, 42). All concentration-response curves were characteristically sigmoidal in nature as analyzed by using curve fitting software (Biosoft UltraFit V1.03 or GraphPad Prism, V2.0a) employing the “built-in” equation for sigmoidal/logistic concentration-response curve fitting; $y = (A_1 - A_2) / [1 + (x/x_0)^n] + A_2$. Consistent with previous findings (38, 42), a subclass of inhibitors where observed in the present study to be effective over a narrow concentration range and inhibited total enzyme activity (e.g. 4, 23, 26, 35, 35) whereas others, despite being potent, were incomplete inhibitors (e.g. 3, 15, 16, 17). The mechanistic basis for this is not fully understood although a selection of compounds from both groups have been shown to be specific, competitive, and reversible inhibitors at the NOS H_4 Bip site (see Ref. 38). As previously, we therefore defined the IC_{50} value in the present study as the concentration of inhibitor required to produce half-maximal enzyme inhibition that can be achieved by each compound. The apparent lack of potency of the inhibitors is to some extent assay related since in our standard “functional” assay, we use a concentration of H_4 Bip (2 μ M) that is in excess in relation to the EC_{50} of H_4 Bip (50–100 nM) for enzyme activation and saturation. However, in radioligand binding studies, we and others (e.g. Ref. 41) have seen a quantitatively different picture with K_i values in the low nanomolar range when using an amount of [3 H] H_4 Bip at the K_d from saturation experiments (about 10 nM).

coordinate files retrieved were from the National Brookhaven PDB data base (52) all hydrogens were added, while structurally conserved water and a glycerol molecule close to the H₄Bip-binding site were removed. All proteins were superimposed using C α atoms of homolog residues around the heme and H₄Bip-binding sites plus selected carbon atoms from heme and H₄Bip.

After analysis of key protein-ligand interactions using the program GRID (53), candidate molecules were manually docked into the active site. The protein-ligand complex was then minimized by treating all ligand atoms plus all protein residues within a sphere of 4 Å as flexible, while the remaining receptor was used to compute non-bonded interactions. Convergence criteria were set to 0.001 kcal Å⁻¹. All related compounds were built accordingly, docked into the NOS-III H₄Bip-binding site and minimized using a flexible receptor.

The program MOLCAD was used for visualization of protein-ligand interactions (54, 55). Molecular properties such as the lipophilicity potential (56–58) and the electrostatic potential (by solving the Poisson-Boltzmann equation; 59–62) were mapped onto Connolly solvent accessible surfaces (63, 64) of the binding site to analyze relevant factors for protein-ligand recognition. The separated surface approach (65) was used to study the properties of the interface between individual ligands and the protein cavity. A separated surface is defined by a set of points located at the midpoint of the shortest distance vectors between surface points of both molecules. Default settings for surface parameters were applied. The step width for the grid to compute the Poisson-Boltzmann electrostatic potential was set to 1 Å, while the border width of the solvent grid around the molecule was set to 8 Å. Dielectric constants of 80 for the solvent and 2 for the solute were used while the electrostatic potential at the boundary was computed using the Debye-Hückel equation.

To obtain more information about H₄Bip-binding site differences in different NOS isoforms, a homology model for the neuronal NOS isoform was generated using the program Composer (66–68) in the Sybyl 6.5 implementation. The x-ray structures of NOS-III and NOS-II isoform dimers (PDB codes 1nod, 2nod, 3nod, 1nse, 3nse, 4nse; Refs. 15, 23, and 50) were used as homologous sequences, while for loop searching and construction the Sybyl 6.5 version of the Brookhaven Protein Data bank with 1495 protein structures was utilized. Initial sets of residues, which are topologically equivalent across the entire family of input structures, were identified based on sequence homology. Then a multiple alignment on the homologous sequences was generated and identities across all sequences and these positions were assigned relative weights proportional to the square of their percentage sequence identity to the model sequence. The weights determine the relative contribution of each homolog to the framework on which the model is built (69). A structural alignment of the known structures using seed residues as the starting point was performed, leading to the determination of structurally conserved regions (SCRs). The sequence (human brain NOS-I, GenBank™ accession code L02881) was aligned with the SCRs to determine the location of the SCRs in the target sequence and the homolog to use in constructing the backbone of each SCR in the final model. This led to a complete model of the structurally conserved regions of the target protein. A fragment from one of the homologs was used to model the backbone of each SCR, while a rule-based procedure was used to model side chains. The structurally variable regions of the target protein was then constructed by selecting a fragment to model each loop region either from the corresponding location in a homologous protein or from the entire protein data base. The final NOS-I monomer was checked for steric overlap, superimposed onto other isoforms and completed by adding heme, H₄Bip, and another NOS-I monomer according to the NOS-III and NOS-II dimerization pattern. Finally, the H₄Bip/NOS-I dimer model was minimized by treating all H₄Bip and heme atoms plus all binding site residues within a sphere of 4 Å as flexible.

Co-crystallization of NOS-III Oxygenase Domain: 1 and 21f (from Ref. 42)—Pterin-free NOS-III heme domain was obtained following expression in *Escherichia coli* (15) and was used for co-crystallization studies with the anti-pterins. Typically, co-crystallization experiments involved the addition of 1–3 mM of the pterin-based inhibitors, **1** or **21f** (from Ref. 42), as previously described (15). Diffraction data were collected under cryogenic conditions (100 K) using synchrotron x-ray source. A Quantum-4 CCD detector (ALS, BL 5.0.2) or Mar imaging plate (SSRL, BL 7–1) was used for data collection. Data were processed with DENZO/SCALEPACK (70). The $F_o - F_c$ difference density, calculated with the pterin-free NOS-III heme domain model as F_c and phases, provided a clear contour of the anti-pterin compounds which afforded model building with TOM (71). Structure refinements were performed using the new maximum likelihood algorithm implemented

in CNS (72). In the case of the **21f** (Ref. 42) complex, the model was refined to a crystallographic $r = 0.225$ ($R_{\text{free}} = 0.265$) against a set of 1.9 Å data (73472 unique reflections with a scaling $R_{\text{sys}} = 0.052$), whereas for the anti-pterin **1** data (40567 unique reflections, $R_{\text{sym}} = 0.047$) at 2.35 Å, the final model had an $r = 0.187$ ($R_{\text{free}} = 0.228$).

RESULTS AND DISCUSSION

We systematically screened and developed a novel class of 4-oxo-pteridine-based NOS inhibitors as drug candidates to therapeutically modulate NOS-mediated pathophysiology. In contrast to previous attempts using 4-amino analogs (anti-pterins) based on the same principle as anti-folates, we synthesized 4-oxo-pteridine derivatives based on the naturally occurring H₄Bip and examined their effects on NOS-I activity. Indeed, analogous to our previous findings (38, 42) a subclass of inhibitors were found to be effective over a narrow concentration range and inhibited total enzyme activity whereas others, despite being potent, were incomplete enzyme inhibitors. As previously, we therefore defined the IC₅₀ value in the present study as the concentration of inhibitor required to produce half-maximal enzyme inhibition that can be achieved by each compound.

NOS Oxygenase Homology Model—To understand the structural requirements for NOS-I inhibition by 4-oxo-pteridines, we determined and compared bioactive conformations for congeneric ligands. Two approaches were used based on the available target homologous protein three-dimensional structures: docking of reference compounds and x-ray crystallography. The docking calculations were based on the availability of three-dimensional x-ray structures for two other, very similar dimeric NOS isoforms solved with bound H₄Bip cofactor; the inducible NOS (NOS-II; Refs. 23 and 50) and the endothelial NOS (NOS-III, Ref. 15). Fig. 1 shows H₄Bip bound within the NOS-III heme dimer at the highest resolution available of 1.9 Å: the pteridine ring lies apparently sandwiched by π -electron stacking between residues Trp⁴⁴⁹ from one monomer and the residue Phe⁴⁶² from the second monomer, and is supported by extensive hydrogen bond networks with Ser¹⁰⁴, Arg³⁶⁷, and the heme propionic acid (see Ref. 15).

Given that no experimental three-dimensional structure for the NOS-I isoform is currently available, for which the herein reported biological affinities have been obtained, this prompted us to additionally derive a homology model for this isoform utilizing the three-dimensional structures and dimerization pattern for both closely related homologs, NOS-III and NOS-II (see Fig. 2: NOS-III in purple, NOS-II in orange, NOS-I in green; the latter being the COMPOSER-derived homology model). Superposition of both experimental NOS structures did not reveal any significant differences in the protein-ligand interaction pattern. While the homology model of NOS-I (green; see Fig. 2) is similar to both experimental structures as templates (15, 23, 50), only two residues in the H₄Bip vicinity differ among these structures: Val¹⁰⁶ (NOS-III) is substituted against Met in NOS-I and NOS-II, while for Ala¹⁴⁸ in NOS-III, an Ile (NOS-II) or Val (NOS-I) replacement is observed, respectively. Thus, the same binding site interactions observed within the crystallized NOS-II and III structures would be directly applicable to the NOS-I used in the present study and any differences in binding affinities among these isoforms can only be explained by small changes in the hydrophobic interaction pattern at the ligand binding surface.

Structural information derived by docking selected inhibitors within the NOS-III heme dimer domain should be applicable to kinetic findings with NOS-I. In support of this, we compared the best docking mode and x-ray structure (see Figs. 3 and 4) for two effective pterin-based NOS inhibitors whose structures are indicated in Fig. 7: the 4-oxo-pteridine **1** described in the present investigation (Table I), and the 4-amino

FIG. 1. Interactions of H₄Bip within the dimeric NOS-III heme dimer domain from the crystal structure. H₄Bip, pink carbon, red oxygen, and blue nitrogen bonds. The pteridine ring is sandwiched by π -electron stacking between Trp⁴⁴⁹ from the first monomer and Phe⁴⁶² (B) from the second monomer. Residues from the first NOS-III monomer are shown in purple, while green indicates residues from the second monomer.

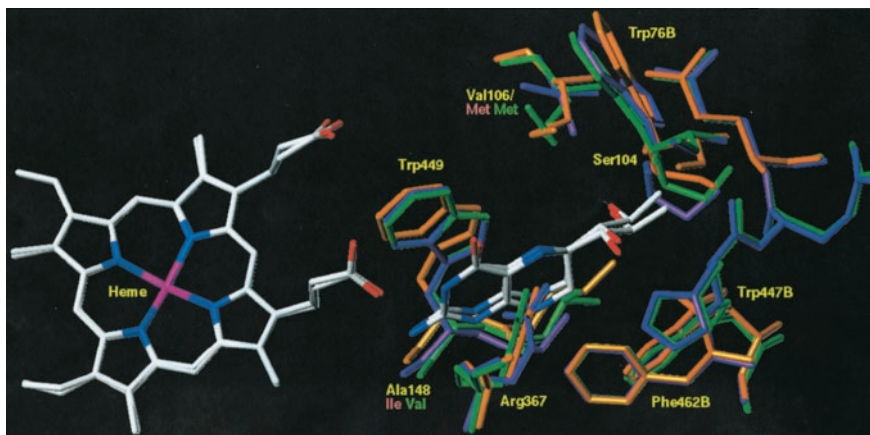
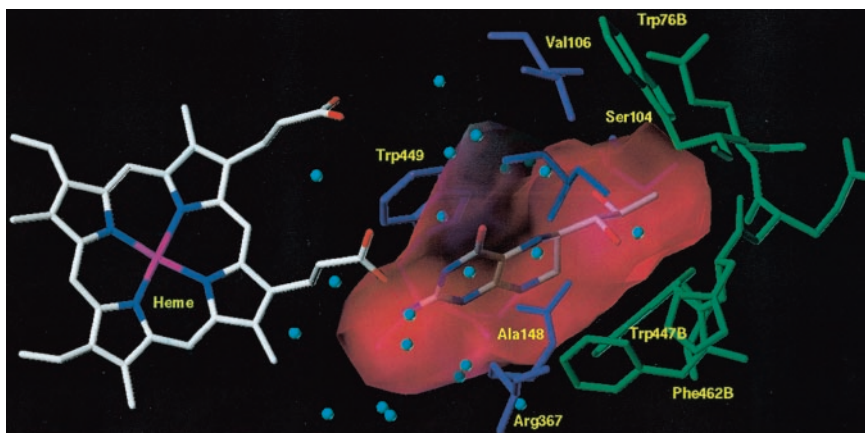


FIG. 2. Structural comparison of different NOS isoform H₄Bip-binding sites including heme moieties. The bound H₄Bip ligand is taken from the NOS-III structure. Residues from NOS-III are shown in purple, NOS-II in orange, and NOS-I in green (COMPOSER-based homology model of the dimer). The interaction surface between H₄Bip and NOS-III is color coded by interaction distance. While the homology model of NOS-I is similar to both experimental structures as templates (15, 23, 50), only two residues in the H₄Bip vicinity differ among these structures: Val¹⁰⁶ (NOS-III) is substituted against Met in NOS-I and NOS-II, while for Ala¹⁴⁸ in NOS-III, an Ile (NOS-II) or Val (NOS-I) replacement is observed, respectively.

pteridine, **21f** from Fröhlich *et al.* (42). In both cases, remarkably similar binding modes were observed when **1** and **21f** were either docked into the NOS-III heme dimer domain (green carbons, see Figs. 3 and 4) or co-crystallized at high resolution within the NOS-III heme dimer domain (white carbons, Figs. 3 and 4). That is, both rings of **1** and **21f** are stacked with 3.6 Å distance and the main interaction occurs between these and the indole of Trp⁴⁴⁹; the hydrogen bonding pattern corresponds to that of bound H₄Bip within NOS (15).

The above structural comparison revealed sequence differences for this inhibitor-binding site raising the possibility of generating isoform selective ligands using *In Silico* “rationale drug design” analogous to that used to discriminate between various target enzymes including COX-1/2 and matrix metalloproteinases (MMP1-MMP23). In the former case, certain key amino acid differences within the active center confer selectivity and have been therapeutically exploited with the development of COX-2-selective ligands (*e.g.* first generation Celebrex and Vioxx). Investigations for isoform selectivity involve a combined approach of structure-based design, homology modeling, and ligand derived structure-activity relationship. For NOS, NOS-I selective ligands appear to have therapeutic advantage in stroke (NOS-III inhibition is detrimental). The detailed sequence and structural comparisons of available and modeled NOS isoform structures revealed two main differences in the binding site, namely the replacement of Val¹⁰⁶ in NOS-III against Met/Met for NOS-I/II and Ala¹⁴⁸ replaced by Ile or Val in NOS-II and III, respectively. Both mutations offer the possibility to design isoform selective inhibitors using the different scaffolds investigated thus far for this binding site. The Val¹⁰⁶ side chain is bulkier and is involved in contact with preferably hydrophobic substituents attached to the 4-, 5-, and 6-positions at the pterin scaffold than the corresponding Met present in

NOS-II and III. In contrast, the latter residue appears to be more flexible, which also may influence protein-ligand interactions in this region. Indeed, we have identified certain 4-amino and 4-oxo-pteridine-based NOS-I inhibitors with appropriate substituents within N-5 and C-6 demonstrating isoform selectivity of up to 30-fold against NOS-II and 10-fold against NOS-III under the same assay conditions.³

Reduced 4-Oxo-pteridine Derivatives and Enzyme Inhibition—We have previously shown that the 6- and 7-positions of the reduced 4-aminopteridine scaffold are important chemical targets in the development of NOS-I inhibitors (42). Here we varied the substitution pattern in the 5-, 6-, and 7-positions of the reduced 4-oxo-pteridine scaffold. This approach yielded several novel compounds that were discovered to inhibit NOS-I activity (see Table I). For example, substituting the 1,2-dihydroxypropyl side chain in the 6-position of the naturally occurring H₄Bip (**1**) with a hydrogen produced a NOS-I inhibitor although with poor efficacy (Table I, compound **2**; residual activity in the presence of 100 μ M inhibitor, $81 \pm 6\%$ of V_{max}). Interestingly, **2** was considerably more active following specific N-5 modifications: acylation with a benzoyl group (**3**, $42 \pm 16\%$ of V_{max} ; $IC_{50} = 90 \mu$ M) and phenylthiocarbamoyl substitution (**4**, $10 \pm 3\%$ of V_{max} ; $IC_{50} = 50 \mu$ M); less effective was a long chain 3-(4-benzoylphenyl)propionyl (**5**, $75 \pm 4\%$ of V_{max}) group and a benzoylthiocarbamoyl (**6**, $78 \pm 7\%$ of V_{max}) substituent. The favorable changes in the case of **3** and **4** may have been due to steric reasons associated with the displacement of structural Arg³⁶⁷ and/or pterin bridging crystal water (15, 23) by the inhibitor within the pterin binding pocket (see Figs. 5 and 6).

³ A. Frey, H. Matter, P. Kotsonis, H. Strobel, O. Klingler, L. G. Fröhlich, W. Pfeleiderer, and H. H. H. W. Schmidt, manuscript in preparation.

FIG. 3. Comparison between the best docking mode (green carbons) and x-ray structure (white carbons) for the 4-oxo-pteridine inhibitor, **1**, in the NOS-III dimer-binding site. Compound **1** was co-crystallized within the NOS-III heme dimer domain (PDB code 1DMJ) as described under “Experimental Procedures.” Residues from the first NOS-III monomer are shown in purple, while green indicate residues from the second monomer.

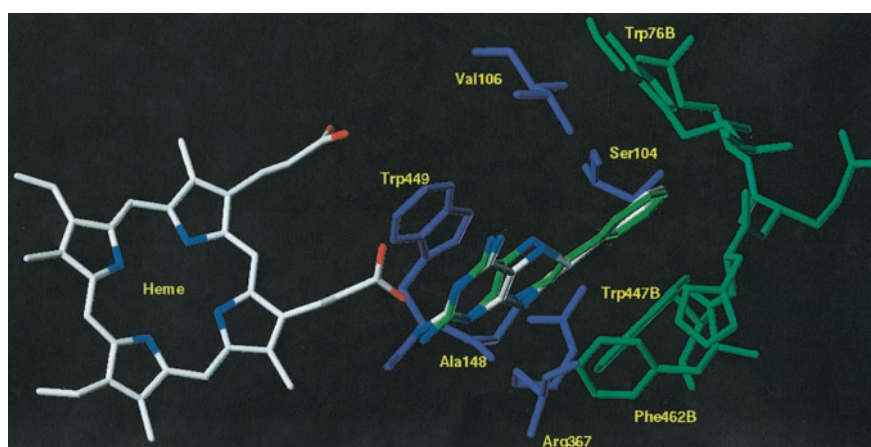
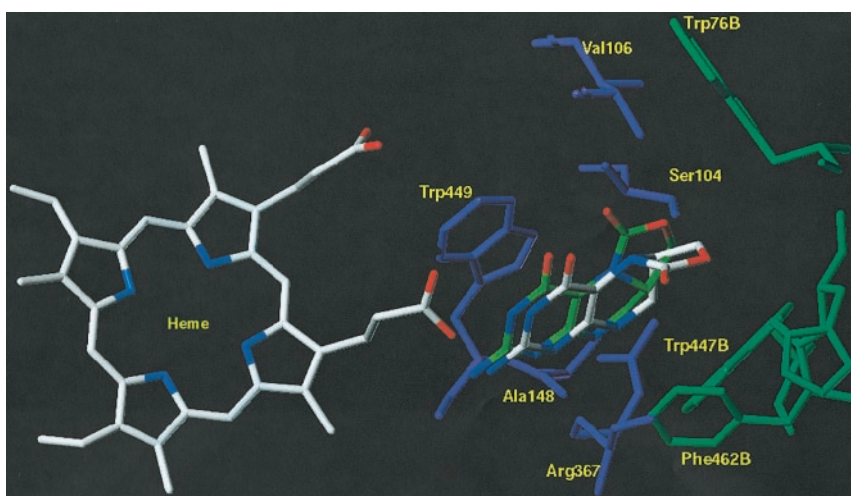


FIG. 4. Comparison between the best docking mode (green carbons) and x-ray structure (white carbons) for the 4-aminopteridine inhibitor, **21f** (from Ref. 42), in the NOS-III dimer-binding site. Compound **21f** was co-crystallized within the NOS-III heme dimer domain (PDB code 1DMK) as described under “Experimental Procedures.” Residues from the first NOS-III monomer are shown in purple, while green indicate residues from the second monomer.

Importantly, the degree of steric tolerance between the N-5 substituted groups and structural Arg³⁶⁷ (and/or pterin bridging crystal water) appeared to be small since, in striking contrast to the active **3** (N-5; -COC₆H₅), the phenoxycarbonyl derivative **7** (N-5; -COOC₆H₅) was devoid of any inhibitory effect on NOS-I activity ($108 \pm 7\%$ of V_{\max}). In this case, the additional bulk due to the bridging oxygen atom probably shifts the phenyl group further away in space and is differently located in relation to the pteridine ring structure.

Differences with respect to steric limitations in the binding mode at the N-5 position probably influence the strength of interactions between the inhibitor and enzyme. For example, while N-5 benzoyl substitution yielded the effective inhibitor **3** ($42 \pm 16\%$ of V_{\max} ; $IC_{50} = 90 \mu\text{M}$), the addition of a *p*-substituted fluorine atom within the benzoyl group rendered this derivative inactive (**8**, Table I; $102 \pm 12\%$ of V_{\max}). We also observed similar results by introducing other electronegative atoms larger in size but less electronegative than fluorine within the *para* position (either *para*-Cl or *para*-I).⁴ Similarly, by substituting additional steric bulk in the 6- and 7-positions of **1** (Table I), modifications at the N-5 position that alone were found to be optimal for inhibition could be effectively counteracted (Table I; compare **3** with **9**, and **4** with **10**). Taken together, the latter findings indicate unfavorable steric hindrance within the pterin binding pocket of NOS-I, possibly involving residues in the first (Ser¹⁰⁴) and second (Phe⁴⁶²) monomers, respectively (Figs. 5 and 6). This contention is consistent with previous molecular modeling using Comparative

Molecular Field Analysis⁴ based on steric and electrostatic considerations and the present docking studies for a selection of active derivatives (Fig. 5).

The above observations prompted us to consider introducing hydrophobic substituents at the 6-position of **1** (Table I) within the region otherwise occupied by the 1,2-dihydroxypropyl side chain of H₄Bip. This should provide ideal steric and hydrophobic complementation to accommodate pterin-binding site interactions with the carbonyl of Ser¹⁰⁴ and the phenyl ring of Phe⁴⁶². Indeed, by substituting a hydrophobic phenyl group at the C-6 position of the otherwise weakly active, 6-unsubstituted **2**, the potent NOS-I inhibitor **11** was generated (Table I; $40 \pm 1\%$ of V_{\max} , $IC_{50} = 7 \mu\text{M}$). In contrast, C-6 substitution with a naphthyl group (**12**; Table I; $67 \pm 16\%$ of V_{\max}) was less effective indicating possibly steric hindrance with Ser¹⁰⁴ and Phe⁴⁶². It is interesting to note that inhibitory potency of **11** was similar to that previously reported (42) with the corresponding 4-amino substituted derivative **21f** ($17 \pm 1\%$ of V_{\max} , $IC_{50} = 6 \mu\text{M}$). This indicates that the 6-position of the reduced 4-oxo-pteridines is also an important chemical target in developing effective NOS-I inhibitors. In general, for the reduced scaffold, the 4-oxo derivatives described within this study displayed similar efficacy and potency to the published 4-amino series (42) when the same substituents were employed under identical assay conditions.

The 1,2-dihydroxypropyl side chain of H₄Bip is known to be important in the activation of NOS and supports high affinity cofactor binding ($K_d = 10\text{--}20 \text{ nM}$) as a consequence of (i), hydrogen bonding with crystal water and/or the carbonyl groups of Ser¹⁰⁴ and Phe⁴⁶² and (ii), hydrophilic and/or hydrophobic interactions with both Ser¹⁰⁴ and Phe⁴⁶² within the

⁴ H. Matter, P. Kotsonis, H. Strobel, O. Klingler, L. G. Fröhlich, W. Pfeleiderer, H. H. H. W. Schmidt, unpublished observations.

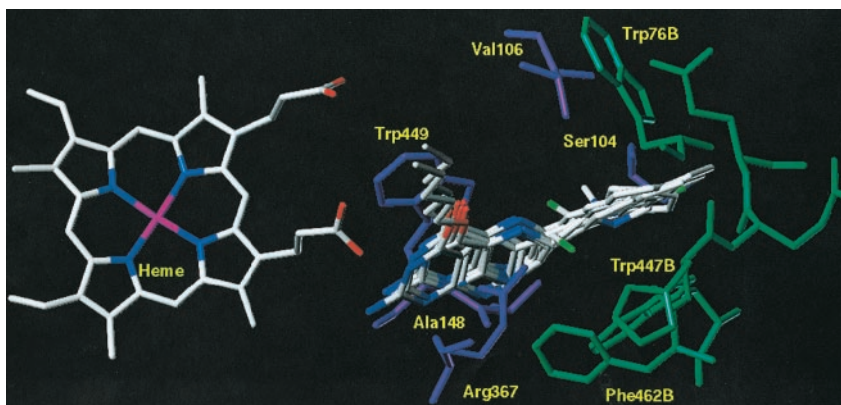
TABLE I
Effect of substituents in the 5, 6, and 7 positions on the inhibition of NOS-I activity by 4-oxo-5,6,7,8-tetrahydropteridine derivatives I

No.	R ₅	R ₆	R ₇	NOS activity ^a	IC ₅₀ ^b
1	CH ₂ OCO (cyclic R ₅ /R ₆)		H	31 ± 6	μ M 35
2	H	H	H	81 ± 6	
3	COC ₆ H ₅	H	H	42 ± 16	90
4	CSNHC ₆ H ₅	H	H	10 ± 3	50
5	CO(CH ₂) ₂ C ₆ H ₄ -4-COC ₆ H ₅	H	H	75 ± 4	
6	CSNHCOC ₆ H ₅	H	H	78 ± 7	
7	COOC ₆ H ₅	H	H	108 ± 7	
8	CO-4-FC ₆ H ₄	H	H	102 ± 12	
9	COC ₆ H ₅	CH ₃	CH ₃	106 ± 2	
10	CSNHC ₆ H ₅	CH ₃	CH ₃	114 ± 8	
11	H	C ₆ H ₅	H	40 ± 1	7
12	H	C ₁₀ H ₇ (Naphthyl-)	H	67 ± 16	
13	H	CH ₂ OH	H	103 ± 5	
14	H	CH ₂ OCH ₃	H	83 ± 3	
15	H	CH ₂ NH ₂	H	44 ± 3	32
16	H	CH ₂ NHCH ₃	H	35 ± 1	20
17	H	CH ₂ N(CH ₃) ₂	H	37 ± 3	25
18	H	CH ₂ OCO(CH ₂) ₂ -C ₆ H ₄ -4-COC ₆ H ₅	H	57 ± 3	

^a Inhibition of H₄Bip (2 μ M) stimulated NOS total activity at an inhibitor concentration of 100 μ M.

^b IC₅₀ values were only determined for those compounds which inhibited NOS total activity at least by 50%.

FIG. 5. Binding modes of the 10 most active 4-oxo-pteridine-based inhibitors docked into the NOS-III dimer-binding site. Inhibitors of IC₅₀ values ranging from 7 to 33 μ M are shown in white carbons, hydrogens are omitted for clarity. Residues from the first NOS-III monomer are shown in purple, while green indicate residues from the second monomer. See Figs. 1 and 2 for further details. The inhibitors shown include: 11, 16, 17, 23, 24, 25, 27, 28, 34, and 35.



pterin pocket (10, 15). To examine further the effect of the 6-position of H₄Bip (**I**, Table I), the 1,2-dihydroxypropyl side chain was either shortened (**13**) or the free hydroxy function of **13** additionally methylated (leading to **14**). However, in both cases this approach failed to produce effective inhibitors (Table I: 103 and 83% of V_{\max} , respectively) whereas replacement of the free hydroxy function of **13** (Table I) with an amino (**15**), methylamino (**16**), or dimethylamino (**17**) functionality led to efficacious NOS inhibitors (Table I; enzyme inhibition, 35–44% of V_{\max} ; IC₅₀ = 20–32 μ M). Moreover, the introduction of a large 3-(4-benzoylphenyl)propionyl substituent at the free hydroxy function was less effective (**18**, 57 ± 34% of V_{\max}). Taken together, these findings apparently indicate (i) a hydrophilic region directly adjacent to the 6-position which can be effectively occupied by both a 1,2-dihydroxypropyl group and CH₂NR₂ substituents (derivatives **15–17**) or (ii) an additional hydrophobic region located further away which can be accessed by substituents in the 6- but not 7-position (see Fig. 5). Consistent with this interpretation, docking studies of the most potent inhibitors based on a reduced 4-oxo-pteridine scaffold (**11**, **16**, and **17**) revealed similar bindings modes as H₄Bip (Fig.

6) with respect to the orientation of the bicyclic framework and favorable steric and hydrophobic interactions at Ser¹⁰⁴ and Phe⁴⁶² with bulky C-6 substituents (Fig. 7 shows the structures of H₄Bip, the 4-oxo-pteridine **1** described in the present investigation in Table I, and the 4-aminopteridine, **21f** from Fröhlich *et al.* (42)).

Aromatic 4-Oxo-pteridine Derivatives and Enzyme Inhibition—We also varied the substitution pattern in the 2-, 4-, 6-, and 7-positions of the corresponding aromatic 4-oxo-pteridine derivatives **II** (Table II). Modifications of the C-6 1,2-dihydroxypropyl side chain of **II** included: shortening the 1,2-dihydroxypropyl side chain (**19**), methylation of the free hydroxy function of **19** (leading to **20**), and substitution of the hydroxy function of **19** with either an amino (**21**) or a dimethylamino (**22**) group. However, in contrast to the reduced 4-oxo-pteridine (**I**) series **15–17** (Table I), in nearly all cases no appreciable enzyme inhibition was observed. We reported similar findings for the same chemical modifications for the corresponding aromatic 4-aminopteridines under identical assay conditions (42) and suggested that their lack of inhibitory potency may be related to the planar conformation of the pyrazine ring and

both ineffective insertion and binding within the H₄Bip cavity. Surprisingly, in contrast to the aromatic 4-aminopteridines (42), 6-phenyl substitution of **II** (Table II) alone markedly increased the inhibitory effectiveness (**23**; $8 \pm 1\%$ of V_{\max} , $IC_{50} = 26 \mu\text{M}$) revealing again functional differences between the 4-oxo- and 4-aminopteridine scaffolds. This appeared to be true also for compounds **24**, **25**, and **26** when compared with the corresponding 4-amino series under identical assay conditions, which were all inactive (see also Ref. 42). These differences probably reflect tighter binding between the 4-oxo-pteridine and NOS-I as a consequence of enhanced hydrophilic interactions between the 4-oxo group with both the propionic acid

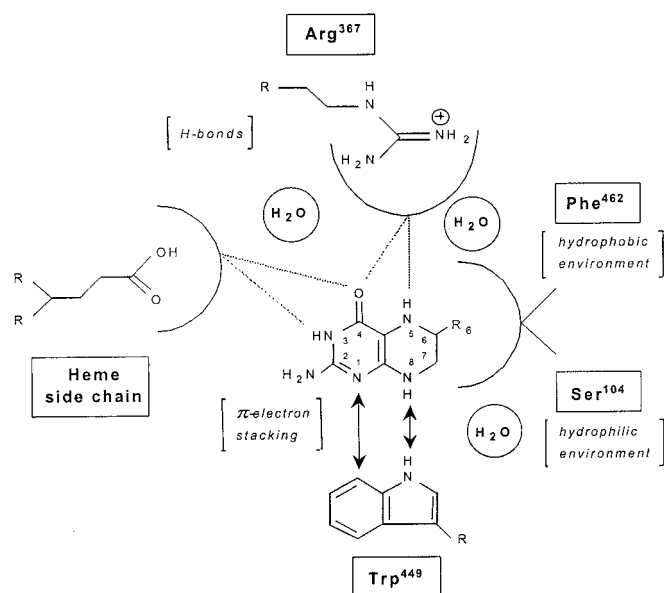


FIG. 6. Two-dimensional representation of possible interactions within the pterin-binding site. The interactions indicated between NOS-I and the reduced 4-oxo-pteridines **I** (Table I; adapted from Ref. 42) would also be applicable for the aromatic 4-oxo-pteridines **II** (Table II).

group of the heme and the iminium group of the guanidine of structural Arg³⁶⁷ (see Figs. 5 and 6).

The introduction of sterically bulky groups in the 6-position of the aromatic 4-oxo-pteridines **II** was found to be an effective approach (Table II; 2–15% of V_{\max} , IC_{50} values = 21–33 μM): 4-chlorophenyl (**24**), 4-methoxyphenyl (**25**), 3-(4-benzoylphenyl)propionyl (**26**), phenylacetyl (**27**), and naphthyl (**28**). It is particularly noteworthy that the aromatic 4-oxo-pteridine scaffold (**II**) appeared to better tolerate additional steric bulk at C-6 compared with the reduced 4-oxo-pteridine series (**I**). This was evident with the C-6 substituents, 3-(4-benzoylphenyl)propionyl (compare **18** with **26**) and a naphthyl (compare **12** with **28**). These differences probably reflect enhanced insertion and binding of the aromatic pyrazine ring within the pterin pocket due to more favorable π -electron stacking with Trp⁴⁴⁹ (see Figs. 5 and 6) as a consequence of the C-6 substitution. In support of this, docking studies revealed similar binding modes between the reduced (Table I; **11**, **16** and **17**) and the aromatic 6-substituted pteridines (Table II; **23**, **24**, **25**, **27**, **28**, **34**, and **35**) regarding: (i) the orientation of the pteridine scaffold between the amino acid residues, Phe⁴⁶² and Trp⁴⁴⁹ and (ii) steric accommodation of C-6 substituents within the region otherwise

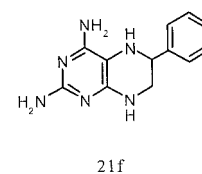
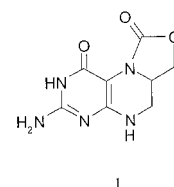
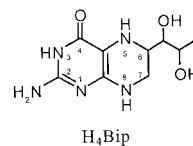


FIG. 7. Structures of H₄Bip compounds **1** (from Table I) and **21f** (from Ref. 42).

TABLE II
Effect of substituents in the 2, 4, 6, and 7 positions on the inhibition of NOS-I activity by aromatic 4-oxo pteridine derivatives **II**

No.	R ₂	R ₄	R ₆	R ₇	NOS activity ^a	IC ₅₀ ^b
						μM
19	NH ₂	H	CH ₂ OH	H	80 ± 10	
20	NH ₂	H	CH ₂ OCH ₃	H	62 ± 9	
21	NH ₂	H	CH ₂ NH ₂	H	81 ± 8	
22	NH ₂	H	CH ₂ N(CH ₃) ₂	H	66 ± 7	
23	NH ₂	H	C ₆ H ₅	H	8 ± 1	26
24	NH ₂	H	4-ClC ₆ H ₄	H	10 ± 3	27
25	NH ₂	H	4-CH ₃ OC ₆ H ₄	H	15 ± 2	29
26	NH ₂	H	CH ₂ OCO(CH ₂) ₂ -C ₆ H ₄ -4-COC ₆ H ₅	H	2 ± 1	60
27	NH ₂	H	CCC ₆ H ₅	H	7 ± 1	21
28	NH ₂	H	C ₁₀ H ₇ (Naphthyl-)	H	13 ± 3	33
29	NH ₂	H	CH ₂ C ₆ H ₅	H	43 ± 3	
30	NHCOCH ₃	H	CH ₂ C ₆ H ₅	H	76 ± 3	
31	NH ₂	H	H	CH ₂ C ₆ H ₅	103 ± 2	
32	NH ₂	CH ₃	H	CH ₂ C ₆ H ₅	120 ± 3	
33	NCN(CH ₃) ₂	H	CH ₂ OCO(CH ₂) ₂ -C ₆ H ₄ -4-COC ₆ H ₅	H	95 ± 2	
34	NH ₂	C ₅ H ₁₁	CCC ₆ H ₅	H	3 ± 0	8
35	NH ₂	C ₅ H ₁₁	CBrCBrC ₆ H ₅	H	9 ± 0	13

^a Inhibition of H₄Bip (2 μM) stimulated NOS total activity at an inhibitor concentration of 100 μM .

^b IC₅₀ values were only determined for those compounds which inhibited NOS total activity at least by 50%.

occupied by the 1,2-dihydroxypropyl side chain of H₄Bip.

Given the steric limitations at the 7-position of **II**, we hypothesize that C-7 substitution would be ineffective on enzyme inhibition analogous with previous results (42) using an aromatic 4-aminopteridine scaffold. This was exemplified by the fact that the favorable inhibitory effect of benzyl substitution in the 6-position of **II** (Table II; **29**, 43 ± 3% of V_{max}) was not observed when substituted in the 7-position (Table II; **31**, 103 ± 2% of V_{max}), probably due to NOS-binding site constraints at Ser¹⁰⁴ and Trp⁴⁴⁹ (Figs. 5 and 6). We found that the 2-position may also influence the inhibitory potential of the aromatic 4-oxo-pteridines since the addition of steric bulk here greatly attenuated the favorable effect of C-6 substitution with either a benzyl (compare **29** and **30**, Table II) or 3-(4-benzoylphenyl)propionyl (compare **26** and **33**, Table II) groups. This finding seems to contrast the situation using the aromatic 4-aminopteridine scaffold (see Ref. 42) where a variety of changes in the 2-position of the pyrimidine moiety, such as replacement of the 2-amino group alone with a hydrogen, methylthio, phenyl, or 2-hydroxyethylamino substituent were without effect. The structural basis for these differences remain to be fully explained although the 2-amino group of H₄Bip interacts via solvent with heme carboxylate and the carbonyl of Trp⁴⁴⁹.

Conclusions—In the present study, 4-oxo-pteridine derivatives of H₄Bip were discovered to inhibit NOS-I activity analogous to the previously described 4-amino analogs and a structure-activity relationship is described. These findings indicate that the 4-amino moiety is not a prerequisite for inhibition and allows for the design of inhibitors with greater selectivity for NOS. Importantly, docking studies of selected 4-oxo-pteridines led to a better understanding of the molecular basis for the ligands' bioactive conformation in relation to biological affinity and was supported by co-crystallization within the largely conserved NOS-III oxygenase domain. The observed binding modes were remarkably similar to H₄Bip with chemical interactions between heme carboxylate and the N-2 amino group, and hydrophobic interactions in the 6-position that are otherwise occupied by the dihydroxypropyl side chain. This information provides a steric and electrostatic basis for the rational design of novel, pteridine-based NOS inhibitors.

Acknowledgments—We thank Manfred Bernhardt and Birgit Thur for excellent technical assistance.

REFERENCES

- Griffith, O. W., and Gross, S. S. (1996) in *Methods in Nitric Oxide Research* (Feelisch, M., and Stamler, J. S., eds) pp. 187–208, John Wiley and Sons, NY
- Hobbs, A. J., Higgs, A., and Moncada, S. (1999) *Annu. Rev. Pharmacol. Toxicol.* **39**, 191–220
- Furchgott, R. F. (1988) in *Vascular Smooth Muscle Peptides, Autonomic Nerves, and Endothelium* (Vanhoutte, P. M., ed) pp. 401–414, Raven, New York
- Ignarro, L. J., Buga, G. M., Wood, K. S., Byrns, R. E., and Chaudhuri, G. (1987) *Proc. Natl. Acad. Sci. U. S. A.* **84**, 9265–9269
- Palmer, R. M. J., Ferrige, A. G., and Moncada, S. (1987) *Nature* **327**, 524–526
- Schmidt, H. H. H. W., Hofmann, H., Schindler, U., Shutenko, Z. S., Cunningham, D. D., and Feelisch, M. (1996) *Proc. Natl. Acad. Sci. U. S. A.* **93**, 14492–14497
- Kotsonis, P., Frey, A., Fröhlich, L. G., Hofmann, H., Reif, A., Wink, D. A., Feelisch, M., and Schmidt, H. H. H. W. (1999) *Biochem. J.* **340**, 745–752
- Komarov, A. M., Wink, D. A., Feelisch, M., and Schmidt, H. H. H. W. (2000) *Free Radic. Biol. Med.* **28**, 739–742
- Schmidt, H. H. H. W., and Walter, U. (1994) *Cell* **78**, 919–925
- Raman, C. S., Martásek, P., and Masters, B. S. S. (2000) in *The Porphyrin Handbook* (Kadish, K. M., Smith, K. M., and Guilard, R., eds) pp. 293–339, Academic Press, New York
- Bredt, D. S., and Snyder, S. H. (1990) *Proc. Natl. Acad. Sci. U. S. A.* **87**, 682–685
- Stuehr, D. J., Cho, H. J., Kwon, N. S., and Nathan, C. F. (1991) *Proc. Natl. Acad. Sci. U. S. A.* **88**, 7773–7777
- Schmidt, H. H. H. W., Smith, R. M., Nakane, M., and Murad, F. (1992) *Biochemistry* **31**, 3243–3249
- Abu-Soud, H. M., Yoho, L. L., and Stuehr, D. J. (1994) *J. Biol. Chem.* **269**, 32047–32050
- Raman, C. S., Li, H., Martásek, P., Král, V., Masters, B. S. S., and Poulos, T. L. (1998) *Cell* **95**, 939–950
- Fischmann, T. O., Hruza, A., Niu, X. D., Fossetta, J. D., Lunn, C. A., Dolphin, E., Prongay, A. J., Reichert, P., Lundell, D. J., Narula, S. K., and Weber, P. C. (1999) *Nat. Struct. Biol.* **6**, 233–242
- Burnett, A. L., Lowenstein, C. J., Bredt, D. S., Cang, K., and Snyder, S. H. (1992) *Science* **257**, 401–403
- Nelson, R. J., Demas, G. E., Huang, P. L., Fishman, M. C., Dawson, V. L., Dawson, T. M., and Snyder, S. H. (1995) *Nature* **378**, 383–386
- Förstermann, U., Pollock, J. S., Schmidt, H. H. H. W., Heller, M., and Murad, F. (1991) *Proc. Natl. Acad. Sci. U. S. A.* **88**, 1788–1792
- Huang, P. L., Huang, Z., Mashimo, H., Bloch, K. D., Bevan, J. A., and Fishman, M. C. (1995) *Nature* **377**, 239–242
- Shesely, E. G., Maeda, N., Kim, H.-S., Desai, K. M., Krege, J. H., Laubach, V. E., Sherman, P. A., Sessa, W. C., and Smithies, O. (1996) *Proc. Natl. Acad. Sci. U. S. A.* **93**, 13176–13181
- MacMicking, J., Xie, Q. W., and Nathan, C. (1997) *Annu. Rev. Immunol.* **15**, 323–350
- Crane, B. R., Arvai, A. S., Ghosh, D. K., Wu, C., Getzoff, E. D., Stuehr, D. J., and Tainer, J. A. (1998) *Science* **279**, 2121–2126
- McCall, T. B., Feelisch, M., Palmer, R. M. J., and Moncada, S. (1991) *Br. J. Pharmacol.* **102**, 234–238
- Olken, N. M., and Marletta, M. A. (1993) *Biochemistry* **32**, 9677–9685
- Huang, H., Martásek, P., Roman, L. J., Masters, B. S. S., and Silverman, R. B. (1999) *J. Med. Chem.* **42**, 3147–3153
- Frey, C., Narayanan, K., McMillan, K., Spack, L., Gross, S. S., Masters, B. S. S., and Griffith, O. W. (1994) *J. Biol. Chem.* **269**, 26083–26091
- Furfine, E. S., Harmon, M. F., Paith, J. E., Knowles, R. G., Salter, M., Kiff, R., Duffy, C., Hazelwood, R., Oplinger, J., and Garvey, E. P. (1994) *J. Biol. Chem.* **269**, 26677–26683
- Narayanan, K., Spack, L., McMillan, K., Kilbourn, R. G., Hayward, M. A., Masters, B. S. S., and Griffith, O. W. (1995) *J. Biol. Chem.* **270**, 11103–11110
- MacDonald, J. E., Shakespeare, W. C., Murray, R. J., and Matz, J. R. (January 25, 1996) Astra AB, Patent WO9601817
- MacDonald, J. E. (August 15, 1996) Astra AB, Patent WO0624588
- Kato, K., Miki, S., Naruo, K.-I., and Takahashi, H. (January 23, 1996) CHEM IND. LTD. Patent EP-0737671-A
- Chabin, R. M., McCauley, E., Calaycay, J. R., Kelly, T. M., MacNaul, K. L., Wolfe, G. C., Hutchinson, N. I., Madhusudanaraju, S., Schmidt, J. A., Kozarich, J. W., and Wong, K. K. (1996) *Biochemistry* **35**, 9567–9575
- Mayer, B., Klatt, E., Werner, E. R., and Schmidt, K. (1994) *Neuropharmacology* **33**, 1253–1259
- Kwon, N. S., Nathan, C. F., and Stuehr, D. J. (1989) *J. Biol. Chem.* **264**, 20496–20501
- Tayeh, M. A., and Marletta, M. A. (1989) *J. Biol. Chem.* **264**, 19654–19658
- Klatt, P., Schmidt, K., Lehner, D., Glatzer, O., Bächinger, H. P., and Mayer, B. (1995) *EMBO J.* **14**, 3687–3695
- Bömmel, H. M., Reif, A., Fröhlich, L. G., Frey, A., Hofmann, H., Marecak, D. M., Groehn, V., Kotsonis, P., La, M., Köster, S., Meinecke, M., Bernhardt, M., Weeger, M., Ghisla, S., Prestwich, G. D., Pfeleiderer, W., and Schmidt, H. H. H. W. (1998) *J. Biol. Chem.* **273**, 33142–33149
- Reif, A., Fröhlich, L. G., Kotsonis, P., Frey, A., Bömmel, H. M., Wink, D. A., Pfeleiderer, W., and Schmidt, H. H. H. W. (1999) *J. Biol. Chem.* **274**, 24921–24929
- Werner, E. R., and Schmidt, H. H. H. W. (2001) *Handbook Exp. Pharmacol.* **143**, 137–158
- Werner, E. R., Pitters, E., Schmidt, K., Werner-Felmayer, G., and Mayer, B. (1996) *Biochem. J.* **320**, 193–196
- Fröhlich, L. G., Kotsonis, P., Traub, H., Taghavi-Moghadam, S., Al-Masoudi, N., Hofmann, H., Strobel, H., Matter, H., Pfeleiderer, W., and Schmidt, H. H. H. W. (1999) *J. Med. Chem.* **42**, 4108–4121
- Boyle, P. H., and Pfeleiderer, W. (1980) *Chem. Ber.* **113**, 1514–1523
- Baugh, C. H., and Shaw, E. (1964) *J. Org. Chem.* **29**, 3610–3612
- Traub, H., and Pfeleiderer, W. (1999) *Pteridines* **10**, 79–90
- Hofmann, H., and Schmidt, H. H. H. W. (1995) *Biochemistry* **34**, 13443–13452
- SYBYL (1999) *Molecular Modelling Package*, Version 6.5, Tripos, St. Louis, MO
- Clark, M., Cramer, R. D., and Van Opdenbosch, N. (1989) *J. Comp. Chem.* **10**, 982–991
- Gasterger, J., and Marsili, M. (1980) *Tetrahedron* **36**, 3219–3228
- Crane, B. R., Arvai, A. S., Gachhui, R., Wu, C., Ghosh, D. K., Getzoff, E. D., Stuehr, D. J., and Tainer, J. A. (1997) *Science* **278**, 425–431
- Brünger, A. T., Adams, P. D., Clore, G. M., DeLano, W. L., Gros, P., Grosse-Kunstleve, R. W., Jiang, J. S., Kuszewski, J., Nilges, M., Pannu, N. S., Read, R. J., Rice, L. M., Simonson, T., and Warren, G. L. (1998) *Acta Crystallogr.* **54**, 905–921
- Brünger, A. T., Adams, P. D., Clore, G. M., DeLano, W. L., Gros, P., Grosse-Kunstleve, R. W., Jiang, J. S., Kuszewski, J., Nilges, M., Pannu, N. S., Read, R. J., Rice, L. M., Simonson, T., and Warren, G. L. (1998) *Acta Cryst.* **54**, 905–921
- Bernstein, F. C., Koetzle, T. F., Williams, G. J. B., Meyer, E. F., Brice, M. D., Rodgers, J. R., Kennard, O., Shimanouchi, T., and Tasoumi, M. (1977) *J. Mol. Biol.* **112**, 535–542
- Goodford, P. J. (1985) *J. Med. Chem.* **28**, 849–857
- Heiden, W., Goetze, T., and Brickmann, J. (1993) *J. Comp. Chem.* **14**, 246–250
- Brickmann, J., Bertling, H., Bussian, B. M., Goetze, T., Knoblauch, M., and Teschner, M. (1987) *Tagungsber. Vortragstag. Ges. Dtsch. Chem., Fachgruppe Chem.-Inf.* 93–111
- Heiden, W., Moeckel, G., and Brickmann, J. (1993) *J. Comp. Aided Mol. Design* **7**, 501–514
- Ghose, A., and Grippen, G. (1986) *J. Comp. Chem.* **7**, 565–577

59. Viswanadhan, V. N., Ghose, A. K., Revankar, G. R., and Robins, R. K. (1989) *J. Chem. Inf. Comput. Sci.* **29**, 163–172
60. Warwicker, J., and Watson, H. (1982) *J. Mol. Biol.* **157**, 671–679
61. Klapper, I., Hagstrom, R., Fine, R., Sharp, K., and Honig, B. (1986) *Proteins* **1**, 47–59
62. Nicholls, A., and Honig, B. (1991) *J. Comp. Chem.* **12**, 435–445
63. Gilson, M., Sharp, K., and Honig, B. (1988) *J. Comp. Chem.* **9**, 327–335
64. Connolly, M. L. (1983) *Science* **221**, 709–713
65. Connolly, M. L. (1983) *J. Appl. Crystallogr.* **16**, 548–558
66. Keil, M., Exner, T. E., and Brickmann, J. (1988) *J. Mol. Mod.* **4**, 335–339
67. Blundell, T. L., Carney, D. P., Gardner, S., Hayes, F. R. F., Howlin, B., Hubbard, T. J. P., Overington, J. P., Singh, D. A., Sibanda, B. L., and Sutcliffe, M. J. (1988) *Eur. J. Biochem.* **172**, 513–520
68. Sutcliffe, M. J., Haneef, I., Carney, D. P., and Blundell, T. L. (1987) *Prot. Eng.* **1**, 377–384
69. Sutcliffe, M. J., Hayes, F. R. F., and Blundell, T. L. (1987) *Prot. Eng.* **1**, 385–392
70. Srinivasan, N., and Blundell, T. (1993) *Protein Eng.* **6**, 501–512
71. Otwinowski, Z., and Minor, W. (1997) *Methods Enzymol.* **276**, 307–326
72. Jones, T. A. (1985) *Methods Enzymol.* **115**, 157–171
73. Katsura, Y., Nishino, S., and Tomishi, T. (January 23, 1997) FUJISAWA PHARM. Co. Ltd., Patent WO9702254